August 2006
hep-ex/0607094
BABAR-PUB-06/010
SLAC-PUB-11968

Measurement of the Pseudoscalar Decay Constant f_{D_s} Using Charm-Tagged Events in e^+e^- Collisions at $\sqrt{s} = 10.58$ GeV

B. Aubert,[1] R. Barate,[1] M. Bona,[1] D. Boutigny,[1] F. Couderc,[1] Y. Karyotakis,[1] J. P. Lees,[1] V. Poireau,[1] V. Tisserand,[1] A. Zghiche,[1] E. Grauges,[2] A. Palano,[3] M. Pappagallo,[3] J. C. Chen,[4] N. D. Qi,[4] G. Rong,[4] P. Wang,[4] Y. S. Zhu,[4] G. Eigen,[5] I. Ofte,[5] B. Stugu,[5] G. S. Abrams,[6] M. Battaglia,[6] D. N. Brown,[6] J. Button-Shafer,[6] R. N. Cahn,[6] E. Charles,[6] C. T. Day,[6] M. S. Gill,[6] Y. Groysman,[6] R. G. Jacobsen,[6] J. A. Kadyk,[6] L. T. Kerth,[6] Yu. G. Kolomensky,[6] G. Kukartsev,[6] G. Lynch,[6] L. M. Mir,[6] P. J. Oddone,[6] T. J. Orimoto,[6] M. Pripstein,[6] N. A. Roe,[6] M. T. Ronan,[6] W. A. Wenzel,[6] M. Barrett,[7] K. E. Ford,[7] T. J. Harrison,[7] A. J. Hart,[7] C. M. Hawkes,[7] S. E. Morgan,[7] A. T. Watson,[7] K. Goetzen,[8] T. Held,[8] H. Koch,[8] B. Lewandowski,[8] M. Pelizaeus,[8] K. Peters,[8] T. Schroeder,[8] M. Steinke,[8] J. T. Boyd,[9] J. P. Burke,[9] W. N. Cottingham,[9] D. Walker,[9] T. Cuhadar-Donszelmann,[10] B. G. Fulsom,[10] C. Hearty,[10] N. S. Knecht,[10] T. S. Mattison,[10] J. A. McKenna,[10] A. Khan,[11] P. Kyberd,[11] M. Saleem,[11] L. Teodorescu,[11] V. E. Blinov,[12] A. D. Bukin,[12] V. P. Druzhinin,[12] V. B. Golubev,[12] A. P. Onuchin,[12] S. I. Serednyakov,[12] Yu. I. Skovpen,[12] E. P. Solodov,[12] K. Yu Todyshev,[12] D. S. Best,[13] M. Bondioli,[13] M. Bruinsma,[13] M. Chao,[13] S. Curry,[13] I. Eschrich,[13] D. Kirkby,[13] A. J. Lankford,[13] P. Lund,[13] M. Mandelkern,[13] R. K. Mommsen,[13] W. Roethel,[13] D. P. Stoker,[13] S. Abachi,[14] C. Buchanan,[14] S. D. Foulkes,[15] J. W. Gary,[15] O. Long,[15] B. C. Shen,[15] K. Wang,[15] L. Zhang,[15] H. K. Hadavand,[16] E. J. Hill,[16] H. P. Paar,[16] S. Rahatlou,[16] V. Sharma,[16] J. W. Berryhill,[17] C. Campagnari,[17] A. Cunha,[17] B. Dahmes,[17] T. M. Hong,[17] D. Kovalskyi,[17] J. D. Richman,[17] T. W. Beck,[18] A. M. Eisner,[18] C. J. Flacco,[18] C. A. Heusch,[18] J. Kroseberg,[18] W. S. Lockman,[18] G. Nesom,[18] T. Schalk,[18] B. A. Schumm,[18] A. Seiden,[18] P. Spradlin,[18] D. C. Williams,[18] M. G. Wilson,[18] J. Albert,[19] E. Chen,[19] A. Dvoretskii,[19] D. G. Hitlin,[19] I. Narsky,[19] T. Piatenko,[19] F. C. Porter,[19] A. Ryd,[19] A. Samuel,[19] R. Andreassen,[20] G. Mancinelli,[20] B. T. Meadows,[20] M. D. Sokoloff,[20] F. Blanc,[21] P. C. Bloom,[21] S. Chen,[21] W. T. Ford,[21] J. F. Hirschauer,[21] A. Kreisel,[21] U. Nauenberg,[21] A. Olivas,[21] W. O. Ruddick,[21] J. G. Smith,[21] K. A. Ulmer,[21] S. R. Wagner,[21] J. Zhang,[21] A. Chen,[22] E. A. Eckhart,[22] A. Soffer,[22] W. H. Toki,[22] R. J. Wilson,[22] F. Winklmeier,[22] Q. Zeng,[22] D. D. Altenburg,[23] E. Feltresi,[23] A. Hauke,[23] H. Jasper,[23] B. Spaan,[23] T. Brandt,[24] V. Klose,[24] H. M. Lacker,[24] W. F. Mader,[24] R. Nogowski,[24] A. Petzold,[24] J. Schubert,[24] K. R. Schubert,[24] R. Schwierz,[24] J. E. Sundermann,[24] A. Volk,[24] D. Bernard,[25] G. R. Bonneaud,[25] P. Grenier,[25,*] E. Latour,[25] Ch. Thiebaux,[25] M. Verderi,[25] D. J. Bard,[26] P. J. Clark,[26] W. Gradl,[26] F. Muheim,[26] S. Playfer,[26] A. I. Robertson,[26] Y. Xie,[26] M. Andreotti,[27] D. Bettoni,[27] C. Bozzi,[27] R. Calabrese,[27] G. Cibinetto,[27] E. Luppi,[27] M. Negrini,[27] A. Petrella,[27] L. Piemontese,[27] E. Prencipe,[27] F. Anulli,[28] R. Baldini-Ferroli,[28] A. Calcaterra,[28] R. de Sangro,[28] G. Finocchiaro,[28] S. Pacetti,[28] P. Patteri,[28] I. M. Peruzzi,[28,†] M. Piccolo,[28] M. Rama,[28] A. Zallo,[28] A. Buzzo,[29] R. Capra,[29] R. Contri,[29] M. Lo Vetere,[29] M. M. Macri,[29] M. R. Monge,[29] S. Passaggio,[29] C. Patrignani,[29] E. Robutti,[29] A. Santroni,[29] S. Tosi,[29] G. Brandenburg,[30] K. S. Chaisanguanthum,[30] M. Morii,[30] J. Wu,[30] R. S. Dubitzky,[31] J. Marks,[31] S. Schenk,[31] U. Uwer,[31] W. Bhimji,[32] D. A. Bowerman,[32] P. D. Dauncey,[32] U. Egede,[32] R. L. Flack,[32] J. R. Gaillard,[32] J .A. Nash,[32] M. B. Nikolich,[32] W. Panduro Vazquez,[32] X. Chai,[33] M. J. Charles,[33] U. Mallik,[33] N. T. Meyer,[33] V. Ziegler,[33] J. Cochran,[34] H. B. Crawley,[34] L. Dong,[34] V. Eyges,[34] W. T. Meyer,[34] S. Prell,[34] E. I. Rosenberg,[34] A. E. Rubin,[34] A. V. Gritsan,[35] M. Fritsch,[36] G. Schott,[36] N. Arnaud,[37] M. Davier,[37] G. Grosdidier,[37] A. Höcker,[37] F. Le Diberder,[37] V. Lepeltier,[37] A. M. Lutz,[37] A. Oyanguren,[37] S. Pruvot,[37] S. Rodier,[37] P. Roudeau,[37] M. H. Schune,[37] A. Stocchi,[37] W. F. Wang,[37] G. Wormser,[37] C. H. Cheng,[38] D. J. Lange,[38] D. M. Wright,[38] C. A. Chavez,[39] I. J. Forster,[39] J. R. Fry,[39] E. Gabathuler,[39] R. Gamet,[39] K. A. George,[39] D. E. Hutchcroft,[39] D. J. Payne,[39] K. C. Schofield,[39] C. Touramanis,[39] A. J. Bevan,[40] F. Di Lodovico,[40] W. Menges,[40] R. Sacco,[40] C. L. Brown,[41] G. Cowan,[41] H. U. Flaecher,[41] D. A. Hopkins,[41] P. S. Jackson,[41] T. R. McMahon,[41] S. Ricciardi,[41] F. Salvatore,[41] D. N. Brown,[42] C. L. Davis,[42] J. Allison,[43] N. R. Barlow,[43] R. J. Barlow,[43] Y. M. Chia,[43] C. L. Edgar,[43] M. P. Kelly,[43] G. D. Lafferty,[43] M. T. Naisbit,[43] J. C. Williams,[43] J. I. Yi,[43] C. Chen,[44] W. D. Hulsbergen,[44] A. Jawahery,[44] C. K. Lae,[44] D. A. Roberts,[44] G. Simi,[44] G. Blaylock,[45] C. Dallapiccola,[45] S. S. Hertzbach,[45] X. Li,[45] T. B. Moore,[45] S. Saremi,[45] H. Staengle,[45] S. Y. Willocq,[45] R. Cowan,[46] K. Koeneke,[46] G. Sciolla,[46] S. J. Sekula,[46] M. Spitznagel,[46] F. Taylor,[46] R. K. Yamamoto,[46] H. Kim,[47] P. M. Patel,[47] C. T. Potter,[47] S. H. Robertson,[47] A. Lazzaro,[48] V. Lombardo,[48] F. Palombo,[48] J. M. Bauer,[49] L. Cremaldi,[49] V. Eschenburg,[49] R. Godang,[49]

Submitted to Physical Review Letters

Work supported in part by Department of Energy contract DE-AC02-76SF00515

R. Kroeger,[49] J. Reidy,[49] D. A. Sanders,[49] D. J. Summers,[49] H. W. Zhao,[49] S. Brunet,[50] D. Côté,[50] M. Simard,[50] P. Taras,[50] F. B. Viaud,[50] H. Nicholson,[51] N. Cavallo,[52,‡] G. De Nardo,[52] D. del Re,[52] F. Fabozzi,[52,‡] C. Gatto,[52] L. Lista,[52] D. Monorchio,[52] P. Paolucci,[52] D. Piccolo,[52] C. Sciacca,[52] M. Baak,[53] H. Bulten,[53] G. Raven,[53] H. L. Snoek,[53] C. P. Jessop,[54] J. M. LoSecco,[54] T. Allmendinger,[55] G. Benelli,[55] K. K. Gan,[55] K. Honscheid,[55] D. Hufnagel,[55] P. D. Jackson,[55] H. Kagan,[55] R. Kass,[55] T. Pulliam,[55] A. M. Rahimi,[55] R. Ter-Antonyan,[55] Q. K. Wong,[55] N. L. Blount,[56] J. Brau,[56] R. Frey,[56] O. Igonkina,[56] M. Lu,[56] R. Rahmat,[56] N. B. Sinev,[56] D. Strom,[56] J. Strube,[56] E. Torrence,[56] F. Galeazzi,[57] A. Gaz,[57] M. Margoni,[57] M. Morandin,[57] A. Pompili,[57] M. Posocco,[57] M. Rotondo,[57] F. Simonetto,[57] R. Stroili,[57] C. Voci,[57] M. Benayoun,[58] J. Chauveau,[58] P. David,[58] L. Del Buono,[58] Ch. de la Vaissière,[58] O. Hamon,[58] B. L. Hartfiel,[58] M. J. J. John,[58] Ph. Leruste,[58] J. Malclès,[58] J. Ocariz,[58] L. Roos,[58] G. Therin,[58] P. K. Behera,[59] L. Gladney,[59] J. Panetta,[59] M. Biasini,[60] R. Covarelli,[60] M. Pioppi,[60] C. Angelini,[61] G. Batignani,[61] S. Bettarini,[61] F. Bucci,[61] G. Calderini,[61] M. Carpinelli,[61] R. Cenci,[61] F. Forti,[61] M. A. Giorgi,[61] A. Lusiani,[61] G. Marchiori,[61] M. A. Mazur,[61] M. Morganti,[61] N. Neri,[61] E. Paoloni,[61] G. Rizzo,[61] J. Walsh,[61] M. Haire,[62] D. Judd,[62] D. E. Wagoner,[62] J. Biesiada,[63] N. Danielson,[63] P. Elmer,[63] Y. P. Lau,[63] C. Lu,[63] J. Olsen,[63] A. J. S. Smith,[63] A. V. Telnov,[63] F. Bellini,[64] G. Cavoto,[64] A. D'Orazio,[64] E. Di Marco,[64] R. Faccini,[64] F. Ferrarotto,[64] F. Ferroni,[64] M. Gaspero,[64] L. Li Gioi,[64] M. A. Mazzoni,[64] S. Morganti,[64] G. Piredda,[64] F. Polci,[64] F. Safai Tehrani,[64] C. Voena,[64] M. Ebert,[65] H. Schröder,[65] R. Waldi,[65] T. Adye,[66] N. De Groot,[66] B. Franek,[66] E. O. Olaiya,[66] F. F. Wilson,[66] R. Aleksan,[67] S. Emery,[67] A. Gaidot,[67] S. F. Ganzhur,[67] G. Hamel de Monchenault,[67] W. Kozanecki,[67] M. Legendre,[67] B. Mayer,[67] G. Vasseur,[67] Ch. Yèche,[67] M. Zito,[67] W. Park,[68] M. V. Purohit,[68] A. W. Weidemann,[68] J. R. Wilson,[68] M. T. Allen,[69] D. Aston,[69] R. Bartoldus,[69] P. Bechtle,[69] N. Berger,[69] A. M. Boyarski,[69] R. Claus,[69] J. P. Coleman,[69] M. R. Convery,[69] M. Cristinziani,[69] J. C. Dingfelder,[69] D. Dong,[69] J. Dorfan,[69] G. P. Dubois-Felsmann,[69] D. Dujmic,[69] W. Dunwoodie,[69] R. C. Field,[69] T. Glanzman,[69] S. J. Gowdy,[69] M. T. Graham,[69] V. Halyo,[69] C. Hast,[69] T. Hryn'ova,[69] W. R. Innes,[69] M. H. Kelsey,[69] P. Kim,[69] M. L. Kocian,[69] D. W. G. S. Leith,[69] S. Li,[69] J. Libby,[69] S. Luitz,[69] V. Luth,[69] H. L. Lynch,[69] D. B. MacFarlane,[69] H. Marsiske,[69] R. Messner,[69] D. R. Muller,[69] C. P. O'Grady,[69] V. E. Ozcan,[69] A. Perazzo,[69] M. Perl,[69] B. N. Ratcliff,[69] A. Roodman,[69] A. A. Salnikov,[69] R. H. Schindler,[69] J. Schwiening,[69] A. Snyder,[69] J. Stelzer,[69] D. Su,[69] M. K. Sullivan,[69] K. Suzuki,[69] S. K. Swain,[69] J. M. Thompson,[69] J. Va'vra,[69] N. van Bakel,[69] M. Weaver,[69] A. J. R. Weinstein,[69] W. J. Wisniewski,[69] M. Wittgen,[69] D. H. Wright,[69] A. K. Yarritu,[69] K. Yi,[69] C. C. Young,[69] P. R. Burchat,[70] A. J. Edwards,[70] S. A. Majewski,[70] B. A. Petersen,[70] C. Roat,[70] L. Wilden,[70] S. Ahmed,[71] M. S. Alam,[71] R. Bula,[71] J. A. Ernst,[71] V. Jain,[71] B. Pan,[71] M. A. Saeed,[71] F. R. Wappler,[71] S. B. Zain,[71] W. Bugg,[72] M. Krishnamurthy,[72] S. M. Spanier,[72] R. Eckmann,[73] J. L. Ritchie,[73] A. Satpathy,[73] C. J. Schilling,[73] R. F. Schwitters,[73] J. M. Izen,[74] I. Kitayama,[74] X. C. Lou,[74] S. Ye,[74] F. Bianchi,[75] F. Gallo,[75] D. Gamba,[75] M. Bomben,[76] L. Bosisio,[76] C. Cartaro,[76] F. Cossutti,[76] G. Della Ricca,[76] S. Dittongo,[76] S. Grancagnolo,[76] L. Lanceri,[76] L. Vitale,[76] V. Azzolini,[77] F. Martinez-Vidal,[77] Sw. Banerjee,[78] B. Bhuyan,[78] C. M. Brown,[78] D. Fortin,[78] K. Hamano,[78] R. Kowalewski,[78] I. M. Nugent,[78] J. M. Roney,[78] R. J. Sobie,[78] J. J. Back,[79] P. F. Harrison,[79] T. E. Latham,[79] G. B. Mohanty,[79] H. R. Band,[80] X. Chen,[80] B. Cheng,[80] S. Dasu,[80] M. Datta,[80] A. M. Eichenbaum,[80] K. T. Flood,[80] J. J. Hollar,[80] J. R. Johnson,[80] P. E. Kutter,[80] H. Li,[80] R. Liu,[80] B. Mellado,[80] A. Mihalyi,[80] A. K. Mohapatra,[80] Y. Pan,[80] M. Pierini,[80] R. Prepost,[80] P. Tan,[80] S. L. Wu,[80] Z. Yu,[80] and H. Neal[81]

(The *BABAR* Collaboration)

[1] *Laboratoire de Physique des Particules, F-74941 Annecy-le-Vieux, France*
[2] *Universitat de Barcelona, Facultat de Fisica Dept. ECM, E-08028 Barcelona, Spain*
[3] *Università di Bari, Dipartimento di Fisica and INFN, I-70126 Bari, Italy*
[4] *Institute of High Energy Physics, Beijing 100039, China*
[5] *University of Bergen, Institute of Physics, N-5007 Bergen, Norway*
[6] *Lawrence Berkeley National Laboratory and University of California, Berkeley, California 94720, USA*
[7] *University of Birmingham, Birmingham, B15 2TT, United Kingdom*
[8] *Ruhr Universität Bochum, Institut für Experimentalphysik 1, D-44780 Bochum, Germany*
[9] *University of Bristol, Bristol BS8 1TL, United Kingdom*
[10] *University of British Columbia, Vancouver, British Columbia, Canada V6T 1Z1*
[11] *Brunel University, Uxbridge, Middlesex UB8 3PH, United Kingdom*
[12] *Budker Institute of Nuclear Physics, Novosibirsk 630090, Russia*
[13] *University of California at Irvine, Irvine, California 92697, USA*
[14] *University of California at Los Angeles, Los Angeles, California 90024, USA*
[15] *University of California at Riverside, Riverside, California 92521, USA*

[16] University of California at San Diego, La Jolla, California 92093, USA
[17] University of California at Santa Barbara, Santa Barbara, California 93106, USA
[18] University of California at Santa Cruz, Institute for Particle Physics, Santa Cruz, California 95064, USA
[19] California Institute of Technology, Pasadena, California 91125, USA
[20] University of Cincinnati, Cincinnati, Ohio 45221, USA
[21] University of Colorado, Boulder, Colorado 80309, USA
[22] Colorado State University, Fort Collins, Colorado 80523, USA
[23] Universität Dortmund, Institut für Physik, D-44221 Dortmund, Germany
[24] Technische Universität Dresden, Institut für Kern- und Teilchenphysik, D-01062 Dresden, Germany
[25] Ecole Polytechnique, LLR, F-91128 Palaiseau, France
[26] University of Edinburgh, Edinburgh EH9 3JZ, United Kingdom
[27] Università di Ferrara, Dipartimento di Fisica and INFN, I-44100 Ferrara, Italy
[28] Laboratori Nazionali di Frascati dell'INFN, I-00044 Frascati, Italy
[29] Università di Genova, Dipartimento di Fisica and INFN, I-16146 Genova, Italy
[30] Harvard University, Cambridge, Massachusetts 02138, USA
[31] Universität Heidelberg, Physikalisches Institut, Philosophenweg 12, D-69120 Heidelberg, Germany
[32] Imperial College London, London, SW7 2AZ, United Kingdom
[33] University of Iowa, Iowa City, Iowa 52242, USA
[34] Iowa State University, Ames, Iowa 50011-3160, USA
[35] Johns Hopkins University, Baltimore, Maryland 21218, USA
[36] Universität Karlsruhe, Institut für Experimentelle Kernphysik, D-76021 Karlsruhe, Germany
[37] Laboratoire de l'Accélérateur Linéaire, IN2P3-CNRS et Université Paris-Sud 11, Centre Scientifique d'Orsay, B.P. 34, F-91898 ORSAY Cedex, France
[38] Lawrence Livermore National Laboratory, Livermore, California 94550, USA
[39] University of Liverpool, Liverpool L69 7ZE, United Kingdom
[40] Queen Mary, University of London, E1 4NS, United Kingdom
[41] University of London, Royal Holloway and Bedford New College, Egham, Surrey TW20 0EX, United Kingdom
[42] University of Louisville, Louisville, Kentucky 40292, USA
[43] University of Manchester, Manchester M13 9PL, United Kingdom
[44] University of Maryland, College Park, Maryland 20742, USA
[45] University of Massachusetts, Amherst, Massachusetts 01003, USA
[46] Massachusetts Institute of Technology, Laboratory for Nuclear Science, Cambridge, Massachusetts 02139, USA
[47] McGill University, Montréal, Québec, Canada H3A 2T8
[48] Università di Milano, Dipartimento di Fisica and INFN, I-20133 Milano, Italy
[49] University of Mississippi, University, Mississippi 38677, USA
[50] Université de Montréal, Physique des Particules, Montréal, Québec, Canada H3C 3J7
[51] Mount Holyoke College, South Hadley, Massachusetts 01075, USA
[52] Università di Napoli Federico II, Dipartimento di Scienze Fisiche and INFN, I-80126, Napoli, Italy
[53] NIKHEF, National Institute for Nuclear Physics and High Energy Physics, NL-1009 DB Amsterdam, The Netherlands
[54] University of Notre Dame, Notre Dame, Indiana 46556, USA
[55] Ohio State University, Columbus, Ohio 43210, USA
[56] University of Oregon, Eugene, Oregon 97403, USA
[57] Università di Padova, Dipartimento di Fisica and INFN, I-35131 Padova, Italy
[58] Universités Paris VI et VII, Laboratoire de Physique Nucléaire et de Hautes Energies, F-75252 Paris, France
[59] University of Pennsylvania, Philadelphia, Pennsylvania 19104, USA
[60] Università di Perugia, Dipartimento di Fisica and INFN, I-06100 Perugia, Italy
[61] Università di Pisa, Dipartimento di Fisica, Scuola Normale Superiore and INFN, I-56127 Pisa, Italy
[62] Prairie View A&M University, Prairie View, Texas 77446, USA
[63] Princeton University, Princeton, New Jersey 08544, USA
[64] Università di Roma La Sapienza, Dipartimento di Fisica and INFN, I-00185 Roma, Italy
[65] Universität Rostock, D-18051 Rostock, Germany
[66] Rutherford Appleton Laboratory, Chilton, Didcot, Oxon, OX11 0QX, United Kingdom
[67] DSM/Dapnia, CEA/Saclay, F-91191 Gif-sur-Yvette, France
[68] University of South Carolina, Columbia, South Carolina 29208, USA
[69] Stanford Linear Accelerator Center, Stanford, California 94309, USA
[70] Stanford University, Stanford, California 94305-4060, USA
[71] State University of New York, Albany, New York 12222, USA
[72] University of Tennessee, Knoxville, Tennessee 37996, USA
[73] University of Texas at Austin, Austin, Texas 78712, USA
[74] University of Texas at Dallas, Richardson, Texas 75083, USA
[75] Università di Torino, Dipartimento di Fisica Sperimentale and INFN, I-10125 Torino, Italy
[76] Università di Trieste, Dipartimento di Fisica and INFN, I-34127 Trieste, Italy
[77] IFIC, Universitat de Valencia-CSIC, E-46071 Valencia, Spain
[78] University of Victoria, Victoria, British Columbia, Canada V8W 3P6

[79] Department of Physics, University of Warwick, Coventry CV4 7AL, United Kingdom
[80] University of Wisconsin, Madison, Wisconsin 53706, USA
[81] Yale University, New Haven, Connecticut 06511, USA

(Dated: July 31, 2006)

Using 230.2 fb^{-1} of e^+e^- annihilation data collected with the *BABAR* detector at and near the peak of the $\Upsilon(4S)$ resonance, 489 ± 55 events containing the pure leptonic decay $D_s^+ \to \mu^+\nu_\mu$ have been isolated in charm-tagged events. The ratio of partial widths $\Gamma(D_s^+ \to \mu^+\nu_\mu)/\Gamma(D_s^+ \to \phi\pi^+)$ is measured to be $0.143 \pm 0.018 \pm 0.006$ allowing a determination of the pseudoscalar decay constant $f_{D_s} = (283 \pm 17 \pm 7 \pm 14)$ MeV. The errors are statistical, systematic, and from the $D_s^+ \to \phi\pi^+$ branching ratio, respectively.

PACS numbers: 13.20.He, 14.40.Nd, 14.60.Fg

Measurements of pure leptonic decays of charmed pseudoscalar mesons are of particular theoretical importance. They provide an unambiguous determination of the overlap of the wavefunctions of the heavy and light quarks within the meson, represented by a single decay constant (f_M) for each meson species (M). The partial width for a D_s^+ meson to decay to a single lepton flavor (l) and its accompanying neutrino (ν_l), is given by

$$\Gamma(D_s^+ \to l^+\nu_l) = \frac{G_F^2|V_{cs}|^2}{8\pi} f_{D_s}^2 m_l^2 m_{D_s} \left(1 - \frac{m_l^2}{m_{D_s}^2}\right)^2, \quad (1)$$

where m_{D_s} and m_l are the D_s^+ and lepton masses, respectively, G_F is the Fermi constant, and V_{cs} is the CKM matrix element giving the coupling of the weak charged current to the c and s quarks [1]. The partial width is governed by two opposing terms in m_l^2. The first term reflects helicity suppression in the decay of the spin-0 meson, requiring the charged lepton to be in its unfavored helicity state. The second term is a phase-space factor. As a result, the ratio of $\tau : \mu : e$ decays is approximately $10 : 1 : 0.00002$. Lattice calculations have resulted in $f_{D_s} = (249 \pm 17)$ MeV and a ratio $f_{D_s}/f_D = 1.24 \pm 0.07$ [2]. CLEO-c has recently measured a value for $f_D = (223 \pm 17)$ MeV [3].

We present herein the most precise measurement to date of the ratio $\Gamma(D_s^+ \to \mu^+\nu_\mu)/\Gamma(D_s^+ \to \phi\pi^+)$ and the decay constant f_{D_s}. The data (230.2 fb^{-1}) were collected with the *BABAR* detector at the asymmetric-energy e^+e^- storage ring PEP-II at and below the $\Upsilon(4S)$ resonance. The *BABAR* detector is described in detail elsewhere [4]. Briefly, the components used in this analysis are the tracking system composed of a five-layer silicon vertex detector and a 40-layer drift chamber (DCH), the Cherenkov detector (DIRC) for charged π–K discrimination, the CsI(Tl) calorimeter (EMC) for photon and electron identification, and the 18-layer flux return (IFR) located outside the 1.5 T solenoid coil and instrumented with resistive plate chambers for muon identification and hadron rejection.

The analysis proceeds as follows. In order to measure $D_s^+ \to \mu^+\nu_\mu$, the decay chain $D_s^{*+} \to \gamma D_s^+, D_s^+ \to \mu^+\nu_\mu$ is reconstructed from D_s^{*+} mesons produced in the hard fragmentation of continuum $c\overline{c}$ events. The subsequent decay results in a photon, a high-momentum D_s^+ and daughter muon and neutrino, lying mostly in the same hemisphere of the event. Signal candidates are required to lie in the recoil of a fully reconstructed D^0, D^+, D_s^+, or D^{*+} meson (the "tag"), wherein the tag flavor, and hence the expected charge of the signal muon, is uniquely determined. To eliminate signal from B decays, the minimum tag momentum is chosen to be close to the kinematic limit for charm mesons arising from B decays. Tagging in this manner significantly reduces backgrounds, while improving the missing mass resolution of the signal.

Tag candidates are reconstructed in the following modes: $D^0 \to K^-\pi^+(\pi^0), K^-\pi^+\pi^+\pi^-$, $D^+ \to K^-\pi^+\pi^+(\pi^0), K_S^0\pi^+(\pi^0), K_S^0\pi^+\pi^+\pi^-, K^+K^-\pi^+, K_S^0K^+$, $D_s^+ \to K_S^0K^+, \phi\rho^+$, and $D^{*+} \to \pi^+D^0$, with $D^0 \to K_S^0\pi^+\pi^-(\pi^0), K_S^0K^+K^-, K_S^0\pi^0$. Kaons are identified using information from the DCH and the DIRC. Requirements on the vertex probability of the tag decay products are imposed. For each tag mode a signal region and sideband regions in the tag mass distribution are defined. The signal region spans ± 2 standard deviations ($\sigma_{\rm tag}$) around the mean ($\mu_{\rm tag}$), determined from fits to the tag mass distribution in data events. The sidebands extend from 3 to 6 $\sigma_{\rm tag}$ on either side of $\mu_{\rm tag}$ (Fig. 1).

For each event a single tag candidate is chosen and then used in the subsequent analysis. To pick this tag among multiple candidates within an event (there are 1.2 candidates on average in events with at least one candidate) modes of higher purity are preferred. In events where two tag candidates are reconstructed in the same mode, the quality of the vertex fit of the D meson is used as a secondary criterion. After subtracting combinatorial background there are $5 * 10^5$ charm tagged events with a muon amongst the recoiling particles.

The signature of the decay $D_s^{*+} \to \gamma D_s^+$ is a narrow peak in the distribution of the mass difference $\Delta M = M(\mu\nu\gamma) - M(\mu\nu)$ at 143.5 MeV/c^2. The D_s^{*+} signal is reconstructed from a muon and a photon candidate in the recoil of the tag. Muons are identified as non-showering tracks penetrating the IFR. The muon must have a momentum of at least 1.2 GeV/c in the center-of-mass (CM) frame and have a charge consistent with the tag flavor.

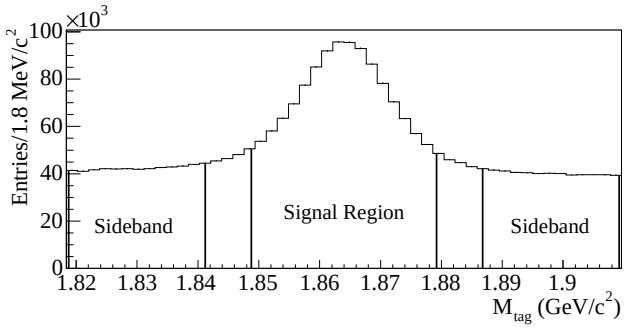

FIG. 1: Tag mass distribution, showing the signal and sideband regions, in events with a recoil muon. All tag modes are combined, scaling their mass and width to that of the $D^0 \to K^-\pi^+$ mode.

Muons used in this analysis are identified with an average efficiency of $\approx 70\,\%$, while the pion misidentification rate is $\approx 2.5\,\%$. Clusters of energy in the EMC not associated with charged tracks are identified as photon candidates. The photon CM energy must exceed 0.115 GeV.

The CM missing energy ($E^*_{\rm miss}$) and momentum ($\vec{p}^{\,*}_{\rm miss}$) are calculated from the four-momenta of the incoming e^+e^-, the tag four-momentum, and the four-momenta of all remaining tracks and photons in the event. The energy of the charged particles that do not belong to the tag is calculated from the track momentum under a pion mass hypothesis. Assigning a mass according to the most likely particle hypothesis has negligible effect on the missing energy resolution. Since the neutrino in the signal decay leads to a large missing energy in the event, the requirement $E^*_{\rm miss} > 0.38$ GeV is made.

The neutrino CM four-momentum ($p^*_\nu = (|\vec{p}^{\,*}_\nu|, \vec{p}^{\,*}_\nu)$) is estimated from the muon CM four-momentum (p^*_μ) and $\vec{p}^{\,*}_{\rm miss}$, using a technique adopted from Ref. [5]. The difference $|\vec{p}^{\,*}_{\rm miss} - \vec{p}^{\,*}_\nu|$ is minimized, while the invariant mass of the neutrino-muon pair is required to be the known mass of the D_s^+ [6]. Studies of simulated decays of signal and background $c\overline{c}$ events show that the quantity $p_{\rm corr} = |\vec{p}^{\,*}_{\rm miss}| - |\vec{p}^{\,*}_\nu|$ is centered at 0 for signal decays, while for the $c\overline{c}$ events it peaks at a negative value significantly separated from the signal. A requirement $p_{\rm corr} > -0.06$ GeV/c is imposed. To reduce contributions from background events where particles are lost along the beam pipe in the forward direction, a requirement on the neutrino CM polar angle $\theta^*_\nu > 38\,^\circ$ is made. The muon CM four-momentum (p^*_μ) is combined with p^*_ν to form the D_s^+ candidate. Unlike the signal D_s^+, a large number of random D_s^+ combinations have the muon candidate aligned with the D_s^+ flight direction. A requirement $\cos(\alpha_{\mu,D_s}) < 0.90$ is made on the angle between the muon direction in the D_s^+ frame and the D_s^+ flight direction in the CM frame. The D_s^+ candidate is then combined with a photon candidate to form the D_s^{*+}. The CM momentum of correctly reconstructed D_s^{*+} is typically higher than that of random combinations; signal candidates are required to have $|\vec{p}^{\,*}_{D_s^{*+}}| > 3.55$ GeV/c. The resulting signal detection efficiency in tagged events is $\epsilon_{\rm Sig} = 8.13\,\%$.

The selection requirements on $E^*_{\rm miss}$, α_{μ,D_s}, $p_{\rm corr}$, θ^*_ν, and $|\vec{p}^{\,*}_{D_s^{*+}}|$ are optimized using simulation to maximize the significance $s/\sqrt{s+b}$, where s and b are the signal and background yields expected in the data set. Backgrounds arise from several distinct sources. The first class of background are events $e^+e^- \to f\bar{f}$, where $f = u, d, s, b$, or τ, which do not contain a real charm tag. The contribution of these events is estimated from data using the tag sidebands. In addition there are events $e^+e^- \to c\overline{c}$ where the tag is incorrectly reconstructed. Although these events potentially contain the signal decay, they are also subtracted using the tag sidebands. These two sources amount to $\approx 42\,\%$ of the background.

The second class of background events ($\approx 26\,\%$) are correctly tagged $c\overline{c}$ events with the recoil muon coming from a semileptonic charm decay or from $\tau^+ \to \mu^+\nu_\mu\bar{\nu}_\tau$. This includes events $D_s^{*+} \to \gamma D_s^+ \to \gamma\tau^+\nu_\tau$, $\tau^+ \to \mu^+\nu_\mu\bar{\nu}_\tau$. To estimate the size and shape of this background contribution, the analysis is repeated, substituting a well-identified electron for the muon. Except for a small phase-space correction, the widths of weak charm decays into muons and electrons are assumed to be equal. QED effects such as bremsstrahlung ($e^+ \to \gamma e^+$) energy losses and photon conversion ($\gamma \to e^+e^-$), where the muon equivalents have a much lower rate, are explicitly removed. In particular, bremsstrahlung photons found in the vicinity of an electron track are combined with the track. The small number of events with an electron from a converted photon that survive the selection are suppressed by a photon conversion veto, using the vertex and the known radial distribution of the material in the detector. The muon selection efficiency as a function of momentum and direction is measured using $e^+e^- \to \mu^+\mu^-\gamma$ events, while radiative Bhabha events are used to quantify the electron efficiency. The ratio of muon to electron efficiencies is applied as a weight to each electron event.

The remaining backgrounds are estimated from simulation. These include events ($\approx 20\,\%$) with pure leptonic decays of a D_s^+ or D^+ meson, $D^+_{(s)} \to \mu^+\nu_\mu$, where the $D^+_{(s)}$ is produced either directly in $c\overline{c}$ fragmentation or in decays of $D^{*+}_{(s)}$, excluding the signal decay chain. If the photon used in the reconstruction originates from a π^0 of a $D^{*+}_{(s)}$ decay, the ΔM distribution peaks sharply around 70 MeV/c^2; otherwise it is flat. A small background ($\approx 1\,\%$) arises from decays $D_s^{*+} \to \gamma D_s^+ \to \gamma\tau^+\nu_\tau$ with $\tau^+ \to \pi^+(\pi^0)\nu_\tau$ and the charged pion being misidentified as a muon. Its ΔM distribution peaks close to that of the signal. Other backgrounds ($\approx 10\,\%$) include signal events with an incorrectly chosen photon candidate, and hadronic $c\overline{c}$ events with one of the final state hadrons,

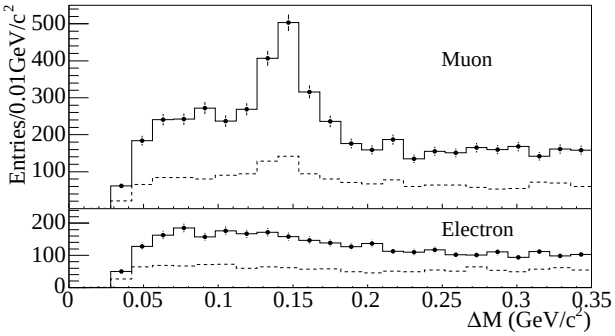

FIG. 2: ΔM distribution of charm-tagged events passing the signal selection. The tag can be from the tag signal region (solid lines) or the sidebands (dashed lines). In the bottom plot the signal muon is replaced with an electron to estimate the semileptonic charm and τ decay background.

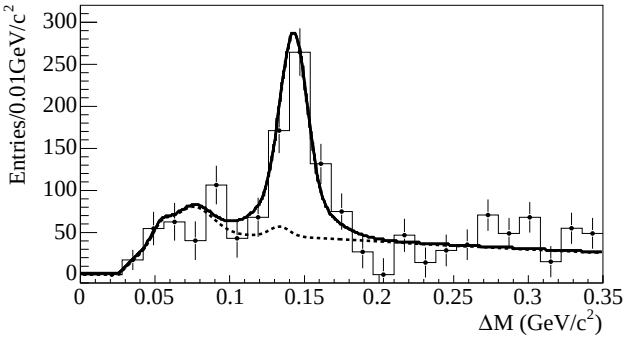

FIG. 3: ΔM distribution after the tag sidebands and the electron sample are subtracted. The solid line is the fitted signal and background distribution ($N_{\rm Sig}f_{\rm Sig} + N_{\rm Bkgd}f_{\rm Bkgd}$), the dashed line is the background distribution ($N_{\rm Bkgd}f_{\rm Bkgd}$) alone.

usually a π^+ or a K^+, being misidentified as a muon. These backgrounds have a flat ΔM distribution.

Events that pass the signal selection are grouped into four sets, depending on whether the tag lies in the signal region or the sideband regions, and on whether the lepton is a muon or an electron (Fig. 2). For each lepton type the sideband ΔM distribution is subtracted. The electron distribution, scaled by the relative phase-space factor (0.97) appropriate to semileptonic charm meson decays and leptonic τ decays is then subtracted from the muon distribution. The resulting ΔM distribution is fitted with a function $(N_{\rm Sig}f_{\rm Sig} + N_{\rm Bkgd}f_{\rm Bkgd})(\Delta M)$, where $f_{\rm Sig}$ and $f_{\rm Bkgd}$ describe the simulated signal and background ΔM distributions. The function $f_{\rm Sig}$ is a double Gaussian distribution. The function $f_{\rm Bkgd}$ consists of a double and a single Gaussian distribution describing the two peaking background components, and a function [7] describing the flat background component. The relative sizes of the background components, along with all parameters except $N_{\rm Sig}$ and $N_{\rm Bkgd}$ are fixed to the values estimated from simulation. The χ^2 fit yields $N_{\rm Sig} = 489 \pm 55(stat)$ signal events and has a fit probability of 8.9 % (Fig. 3).

The branching fraction of $D_s^+ \to \mu^+\nu_\mu$ cannot be determined directly, since the production rate of $D_s^{(*)+}$ mesons in $c\overline{c}$ fragmentation is unknown. Instead the partial width ratio $\Gamma(D_s^+ \to \mu^+\nu_\mu)/\Gamma(D_s^+ \to \phi\pi^+)$ is measured by reconstructing $D_s^{*+} \to \gamma D_s^+ \to \gamma\phi\pi^+$ decays. The $D_s^+ \to \mu^+\nu_\mu$ branching fraction is evaluated using the measured branching fraction for $D_s^+ \to \phi\pi^+$.

Candidate ϕ mesons are reconstructed from two kaons of opposite charge. The ϕ candidates are combined with charged pions to form D_s^+ meson candidates. Both times a geometrically constrained fit is employed, and a minimum requirement on the fit quality is made. The ϕ and the D_s^+ candidate masses must lie within $2\,\sigma$ of their nominal values, obtained from fits to simulated events and data. Photon candidates are then combined with the D_s^+ to form D_s^{*+} candidates. The same requirements on the CM photon energy and D_s^{*+} momentum as in the $D_s^+ \to \mu^+\nu_\mu$ signal selection are made. The $D_s^{*+} \to \gamma D_s^+ \to \gamma\phi\pi^+$ selection efficiency in tagged events is $\epsilon_{\phi\pi} = 9.90\,\%$. Data events that pass the selection are grouped into two sets: the tag signal and sideband regions. After the tag sideband has been subtracted from the tag signal ΔM distribution, the remaining distribution is fitted with $(N_{\phi\pi}f_{\phi\pi}+N_{\phi\pi{\rm Bkgd}}f_{\phi\pi{\rm Bkgd}})(\Delta M)$, where $f_{\phi\pi}$ is a triple Gaussian, describing the simulated $D_s^{*+} \to \gamma D_s^+ \to \gamma\phi\pi^+$ signal, and $f_{\phi\pi{\rm Bkgd}}$ consists of a broad Gaussian centered at 70 MeV/c^2 and a function [7] describing the simulated background ΔM distributions. The Gaussian describes the background $D_s^{*+} \to \pi^0 D_s^+ \to \pi^0\phi\pi^+$ where the photon candidate originates from the π^0. The relative sizes of the background components, along with all parameters except $N_{\phi\pi}$, $N_{\phi\pi{\rm Bkgd}}$, and the mean of the peak are fixed to the values estimated from simulation. The χ^2 fit yields $N_{\phi\pi} = 2093 \pm 99$ events and has a probability of 25.0 % (Fig. 4). From simulation 48 ± 23 events $D_s^{*+} \to \gamma D_s^+ \to \gamma f_0(980)(K^+K^-)\pi^+$ are expected to contribute to the signal, where the error is mostly from the uncertainty in the $D_s^+ \to f_0(980)(K^+K^-)\pi^+$ braching ratio.

Precise knowledge of the efficiency of reconstructing the tag is not important, since it mostly cancels in the calculation of the partial width ratio. However, the presence of two charged kaons in $D_s^+ \to \phi\pi^+$ events leads to an increased number of random tag candidates, compared to $D_s^+ \to \mu^+\nu_\mu$ events, which decreases the chances that the correct tag is picked. The size of the correction for this effect to the efficiency ratio $(\epsilon_{\phi\pi}/\epsilon_{\rm Sig})$ is determined to be $-1.4\,\%$ in simulated events.

To measure the effect of a difference between the D_s^{*+} momentum spectrum in simulated and data events, $D_s^{*+} \to \gamma D_s^+ \to \gamma\phi\pi^+$ events are selected in data with the D_s^{*+} momentum requirement removed. The sample is purified by requiring the CM momentum of the charged

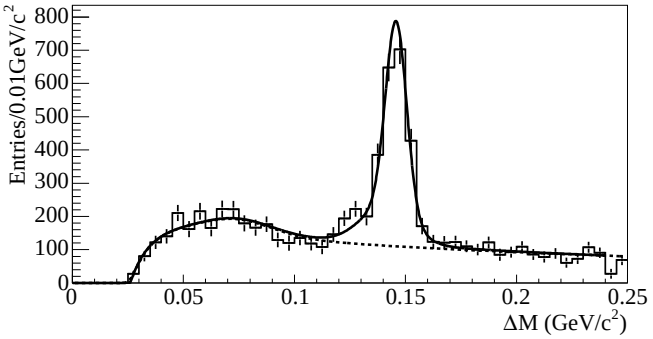

FIG. 4: ΔM distribution of selected $D_s^{*+} \to \gamma D_s^+ \to \gamma\phi\pi^+$ events after the tag sideband is subtracted. The solid line is the fitted signal and background distribution ($N_{\phi\pi} f_{\phi\pi} + N_{\phi\pi\mathrm{Bkgd}} f_{\phi\pi\mathrm{Bkgd}}$), the dashed line is the background distribution ($N_{\phi\pi\mathrm{Bkgd}} f_{\phi\pi\mathrm{Bkgd}}$) alone.

pion to be at least 0.8 GeV/c. The efficiency-corrected D_s^{*+} momentum distribution in data is compared to that of D_s^{*+} in simulated $D_s^{*+} \to \gamma D_s^+ \to \gamma\phi\pi^+$ events. A harder momentum spectrum is observed in data. The detection efficiencies for signal and $D_s^{*+} \to \gamma D_s^+ \to \gamma\phi\pi^+$ events are re-evaluated after weighting simulated events to match the D_s^{*+} momentum distribution measured in data. The correction to the efficiency ratio is $+1.5\,\%$.

With both corrections applied, the partial width ratio is determined to be $\Gamma_{\mu\nu}/\Gamma_{\phi\pi} = (N/\epsilon)_{\mathrm{Sig}}/(N/\epsilon)_{\phi\pi} \times \mathcal{B}(\phi \to K^+K^-) = 0.143 \pm 0.018(stat)$, with $\mathcal{B}(\phi \to K^+K^-) = 49.1\,\%$ [6].

The combined systematic uncertainty due to the corrections applied, taken as half the size of each correction, is $1.0\,\%$. The systematic error in the signal efficiency due to selection criteria insensitive to the D_s^{*+} momentum is evaluated using reconstructed $D^{*0} \to \gamma D^0 \to \gamma K^-\pi^+$ events. The conditions present in the signal are emulated by removing the charged pion, taken to represent the neutrino, from these events. The signal reconstruction and selection steps are repeated, and the selection efficiencies compared between simulated and data events. The assigned systematic uncertainty is $1.4\,\%$. For the $D_s^+ \to \phi\pi^+$ selection, requirements on the D_s^+ and ϕ vertex fit probability contribute a systematic uncertainty of $0.7\,\%$, estimated from comparisons of $D_s^+ \to \phi\pi^+$ events in simulation and data. Control samples of $e^+e^- \to \mu^+\mu^-\gamma$ and $D^{*+} \to \pi^+D^0 \to \pi^+K^-\pi^+$ events are used to measure the particle identification efficiencies of muons and charged kaons and pions in data, and to correct the simulated signal and $D_s^{*+} \to \gamma D_s^+ \to \gamma\phi\pi^+$ efficiencies. An uncertainty of $0.7\,\%$ is associated with these corrections, mainly due to the limited statistics of the control samples. The systematic uncertainties in the track reconstruction efficiency cancel partially in the $D_s^+ \to \mu^+\nu_\mu$ to $D_s^+ \to \phi\pi^+$ ratio and contribute $1.2\,\%$. An additional uncertainty of $1.1\,\%$ is due to the statistical limitations of the simulated signal and $D_s^+ \to \phi\pi^+$ event samples. Simulation studies are used to evaluate the systematic uncertainties arising from a possible inadequate parameterization of the signal ($0.9\,\%$) and background ($2.3\,\%$) shapes. Simulations are also used to determine the systematic uncertainty associated with the subtraction of the electron sample ($0.4\,\%$). The error on the branching ratio $\mathcal{B}(\phi \to K^+K^-)$ is $1.2\,\%$, the uncertainty on the $D_s^+ \to f_0(980)\pi^+$ background is $1.1\,\%$. The total systematic uncertainty on $\Gamma(D_s^+ \to \mu^+\nu_\mu)/\Gamma(D_s^+ \to \phi\pi^+)$ is $3.9\,\%$.

Using the *BABAR* average for the branching ratio $\mathcal{B}(D_s^+ \to \phi\pi^+) = (4.71 \pm 0.46)\,\%$ [8][9], we obtain the branching fraction $\mathcal{B}(D_s^+ \to \mu^+\nu_\mu) = (6.74 \pm 0.83 \pm 0.26 \pm 0.66) \times 10^{-3}$ and the decay constant $f_{D_s} = (283 \pm 17 \pm 7 \pm 14)$ MeV. The first and second errors are statistical and systematic, respectively; the third is the uncertainty from $\mathcal{B}(D_s^+ \to \phi\pi^+)$. The ratio of our value for f_{D_s} to f_D from the CLEO-c measurement, $f_{D_s}/f_D = 1.27 \pm 0.14$, is consistent with lattice QCD.

Using $\mathcal{B}(D_s^+ \to \phi\pi^+)_{\mathrm{PDG}} = (3.6 \pm 0.9)\,\%$ [6], the branching fraction is $\mathcal{B}(D_s^+ \to \mu^+\nu_\mu) = (5.15 \pm 0.63 \pm 0.20 \pm 1.29) \times 10^{-3}$ and the decay constant $f_{D_s} = (248 \pm 15 \pm 6 \pm 31)$ MeV.

We are grateful for the excellent luminosity and machine conditions provided by our PEP-II colleagues, and for the substantial dedicated effort from the computing organizations that support *BABAR*. The collaborating institutions wish to thank SLAC for its support and kind hospitality. This work is supported by DOE and NSF (USA), NSERC (Canada), IHEP (China), CEA and CNRS-IN2P3 (France), BMBF and DFG (Germany), INFN (Italy), FOM (The Netherlands), NFR (Norway), MIST (Russia), and PPARC (United Kingdom). Individuals have received support from the Marie Curie EIF (European Union) and the A. P. Sloan Foundation.

* Also at Laboratoire de Physique Corpusculaire, Clermont-Ferrand, France
† Also with Università di Perugia, Dipartimento di Fisica, Perugia, Italy
‡ Also with Università della Basilicata, Potenza, Italy

[1] Charge conjugation is implied throughout this Letter.
[2] C. Aubin *et al.*, Phys. Rev. Lett. **95**, 122002 (2005).
[3] CLEO Collaboration, M. Artuso *et al.*, Phys. Rev. Lett. **95**, 251801 (2005).
[4] *BABAR* Collaboration, B. Aubert *et al.*, Nucl. Instrum. Methods Phys. Res., Sect. A **479**, 1 (2002).
[5] CLEO Collaboration, M. Chadha *et al.*, Phys. Rev. D **58**, 032002 (1998).
[6] Particle Data Group, S. Eidelman *et al.*, Phys. Lett. B **592**, 1 (2004).
[7] $\bar{A}(\Delta M|\Delta M_0, a, b, c) = \left(1 - \exp\left(-\frac{\Delta M - \Delta M_0}{c}\right)\right)\left(\frac{\Delta M}{\Delta M_0}\right)^a + b\left(\frac{\Delta M}{\Delta M_0} - 1\right)$.
[8] *BABAR* Collaboration, B. Aubert *et al.*, Phys. Rev. D **71**,

091104 (2005).
[9] *BABAR* Collaboration, B. Aubert *et al.*, hep-ex/0605036, to appear in Phys. Rev. D - Rapid Communications.